The Effect of Calcination Temperature on the Surface Microstructure and Photocatalytic Activity of TiO_2 Thin Films Prepared by Liquid Phase Deposition

Jia-Guo Yu,*,† Huo-Gen Yu,† Bei Cheng,‡ Xiu-Jian Zhao,‡ Jimmy C. Yu,§ and Wing-Kei Ho§

State Key Laboratory of Advanced Technology for Material Synthesis and Processing, and Key Laboratory for Silicate Materials and Engineering of Ministry of Education, Wuhan University of Technology, Wuhan, 430070, P. R. of China, and Department of Chemistry, The Chinese University of Hong Kong, Shatin, New Territories, Hong Kong, China

Received: July 23, 2003; In Final Form: October 14, 2003

TiO_2 thin films were prepared on fused quartz by the liquid-phase deposition (LPD) method from a $(NH_4)_2TiF_6$ aqueous solution upon addition of boric acid (H_3BO_3) and calcined at various temperatures. The as-prepared films were characterized with thermogravimetry (TG), Fourier transform infrared spectra (FTIR), X-ray diffraction (XRD), UV−Visible spectrophotometry (UV−Vis), scanning electron microscopy (SEM), photoluminescence spectra (PL), and X-ray photoelectron spectroscopy (XPS), respectively. The photocatalytic activity of the samples was evaluated by photocatalytic decolorization of methyl orange aqueous solution. It was found that the as-prepared TiO_2 thin films contained not only Ti and O elements, but also a small amount of F, N, and Si elements. The F and N came from the precursor solution, and the amount of F decreased with increasing calcination temperature. Two sources of Si were identified. One was from the SiF_6^{2-} ions, which were formed by a reaction between the treatment solution and quartz substrate. The other was attributed to the diffusion of Si from the surface of quartz substrate into TiO_2 thin film at 700 °C or higher calcination temperatures. With increasing calcination temperature, the photocatalytic activity of the TiO_2 thin films gradually increased due to the improvement of crystallization of the anatase TiO_2 thin films. At 700 °C, the TiO_2 thin film showed the highest photocatalytic activity due to the increasing amount of SiO_2 as an adsorbent center and better crystallization of TiO_2 in the composite thin film. Moreover, the SiO_2/TiO_2 composite thin film showed the lowest PL intensity due to a decrease in the recombination rate of photogenerated electrons and holes under UV light irradiation, which further confirms the film with the highest photocatalytic activity at 700 °C. When the calcination temperature is higher than 700 °C, the decrease in photocatalytic activity is due to the formation of rutile and the sintering and growth of TiO_2 crystallites resulting in the decrease of surface area.

1. Introduction

A number of investigations have focused on the semiconductor photocatalyst for its applications in solar energy conversion and environmental purification since Fujishima and Honda discovered the photocatalytic splitting of water on the TiO_2 electrodes in 1972.[1−11] Among various oxide semiconductor photocatalysts, titania is a very important photocatalyst for its strong oxidizing power, nontoxicity, and long-term photostability. To avoid the use of powder, which has to be separated from the water in a slurry system after photocatalytic reaction, many researchers have been developing various ways to apply TiO_2 coatings on various substrates. It is well-known that the photocatalytic activity of TiO_2 thin films strongly depends on the preparing methods and posttreatment conditions, since they have a decisive influence on the chemical and physical properties of TiO_2 thin films.[12,13] Therefore, it is necessary to elucidate the influence of the preparation process and posttreatment conditions on the photocatalytic activity and surface microstructures of the films.

The TiO_2 thin films are usually prepared by vacuum evaporation, sputtering, chemical vapor deposition (CVD), and the sol−gel method. However, these methods have some disadvantages for industry applications. Vacuum evaporation, sputtering, and chemical vapor deposition methods require special apparatuses for deposition of films, and the sol−gel method needs coating repeatedly in order to get thick films. A new process called liquid-phase deposition (LPD) has been developed to form titanium dioxide thin films since 1988.[14−19] The LPD process consists of a ligand exchange equilibrium reaction of the metal-fluorocomplex ions [eq 1] and F^- ions consuming reaction by boric acid as a F^- scavenger [eq 2].[20,21]

$$[TiF_6]^{2-} + nH_2O \rightleftharpoons [TiF_{6-n}(OH)_n]^{2-} + nHF \qquad (1)$$

$$H_3BO_3 + 4HF \rightleftharpoons HBF_4 + 3H_2O \qquad (2)$$

H_3BO_3 reacts readily with F^- ions to form the more stable BF_4^- ions, which promotes the consumption of noncoordinated F^- ions.[22,23] In this process, it is possible to form a titania thin film on the substrate which is immersed in the treatment solution for deposition. The LPD method is very simple and does not require any special equipment. Moreover, it is easily applied to

* Author to whom correspondence should be addressed. E-mail: yujiaguo@public.wh.hb.cn.

† State Key Laboratory of Advanced Technology for Material Synthesis and Processing, Wuhan University of Technology.

‡ Key Laboratory for Silicate Materials and Engineering of Ministry of Education, Wuhan University of Technology.

§ The Chinese University of Hong Kong.

10.1021/jp036158y CCC: $25.00 © 2003 American Chemical Society
Published on Web 11/20/2003

various kinds of substrates with a large surface area or complex morphology.

In the present work, we have prepared titania thin films on fused quartz from $(NH_4)_2TiF_6$ aqueous solution upon addition of boric acid by the liquid-phase deposition (LPD) method. The as-prepared TiO_2 films were then calcined at a different temperature. This is the first report on the effects of calcination temperature on the surface microstructures and photocatalytic activity of TiO_2 thin films obtained by LPD method. This work may provide new insights for preparing highly photocatalytic activity TiO_2 thin films.

2. Experimental Section

2.1. Preparation. Aqueous solutions of ammonium hexafluorotitanate and boric acid were mixed, stirred, and used as treatment solution. The resultant concentration of treatment solution was 0.1 mol L^{-1} for ammonium hexfluorotitanate and 0.3 mol L^{-1} for boric acid, which are in the concentration range where transparent films can be obtained.[24] If the solution is highly supersaturated, precipitation takes place dominantly through homogeneous nucleation. On the contrary, the solution is metastable because of an extremely low reaction rate. Film formation through heterogeneous nucleation on the substrates was observed in the intermediate condition between highly supersaturated and metastable. Usually, the small differences in solution concentration, temperature, and pH can lead to different solution supersaturation, which can significantly influence the formation and growth rate of TiO_2 thin films.[16] A molar radio of $[TiF_6]^{2-}/H_3BO_3 = 1:2-4$ is most suitable for the formation of thin films. If the concentration of H_3BO_3 is low, the noncoordinated F^- ions in the solution cannot be effectively scavenged and the hydrolysis of $[TiF_6]^{2-}$ would be difficult. Furthermore, if the concentration of $[TiF_6]^{2-}$ ions is lower than 0.05 mol L^{-1}, the deposition time will be very long due to an extremely low reaction rate because of low supersaturation. On the contrary, precipitation would occur through homogeneous nucleation when the concentration of $[TiF_6]^{2-}$ is over 0.2 mol L^{-1}. The fused quartz substrates (80 mm × 30 mm × 2 mm) were carefully cleaned by using ultrasonic treatment with base, acid aqueous solution, alcohol, and distilled water, and then dried in an oven at 100 °C. The clean substrates were dipped into the treatment solution and suspended there vertically for 48 h. The treatment solution was kept at room temperature (24 °C) and its pH is 3.9. After the substrates were taken out and rinsed with distilled water, the TiO_2 thin films were calcined at 100, 300, 400. 500. 600, 700, 800 and 900 °C in air for 1 h, respectively. The TiO_2 thin films deposited on the quartz surfaces by LPD method showed strong adhesion in the Scotch tape adhesion peel test. Peeled fragments were not detected. The films were intact even after ultrasonication (in a 100 W cleaning bath) for as long as 20 min. The strong adhesion of films on the quartz was attributed to the chemical bonds formed between TiO_2 precursor particles and OH groups of quartz surfaces by condensation. With increasing calcination temperatures, there are much more chemical bonds produced due to the enhancement of condensation reaction, resulting in stronger adhesion.

Apart from the above-described thin film samples, powder samples were also prepared under the same reaction conditions as the thin films and calcined at the same temperature of thin films samples.

2.2. Characterization. The X-ray diffraction (XRD) patterns obtained on HZG41B-PC X-ray diffractometer using Cu Kα radiation at a scan rate of 0.05° 2θ S^{-1} were used to determine the identity of crystalline phase and their crystallite size. The accelerating voltage and the applied current are 35 kV and 20 mA, respectively. UV−Vis transmittance and reflectance spectra of titania thin films were obtained using a UV−Visible spectrophotometer (UV-1601, Japan). $BaSO_4$ was used as a reflectance standard in the UV−Vis diffuse reflectance experiment. The thermogravimetry (TG) was performed using a TG-DTA instrument (Setaram TG-DTA 92−16, France), under an air flow of 100 mL min^{-1} with a heating rate of 10 k min^{-1} from room temperature to 1000 °C. The scanning electron micrographs were obtained on a JSM-5610LV microscope (Japan). Photoluminescence spectra were measured at room temperature on a SHIMADZU RF-5301 PC spectrometer using a 300 nm excitation light. Since the intensity of the emission strongly depended on the measurement conditions, such as, temperature, humidity, the amount of samples, and so on, the conditions were fixed as far as possible in order to compare the intensity of the PL signals. X-ray photoelectron spectroscopy (XPS) measurements were done on a KRATOA XSAM800 XPS system with Mg Kα source. All the binding energies were referenced to the C1s peak at 284.8 eV of the surface adventitious carbon. Infrared absorption spectra were recorded for KBr disks containing powder sample with an FTIR spectrometer (Nialet-60SXB, American).

2.3. Photocatalytic Activity. The photocatalytic activity evaluation of TiO_2 thin films for the photocatalytic decolorization of methyl orange aqueous solution was performed at ambient temperature. Experiments were as follows: TiO_2 thin films were settled in a 25 mL methyl orange aqueous solution with a concentration of 1.53×10^{-3} mol L^{-1} in a cell (60 mm × 160 mm × 30 mm). The area of the film photocatalyst used for each experiment was kept at about 80 cm^2. A 15-W 365 nm UV lamp (Cole-Parmer Instrument Co.) was used as a light source. One face of the TiO_2 thin films was irradiated along the normal direction. The average light intensity striking on the TiO_2 film was about 112 μW cm^{-2}, as measured by a UV meter (made in the photoelectric instrument factory of Beijing normal university) with the peak intensity of 365 nm. The concentration of methyl orange was determined by a UV−visible spectrophotometer. As for the methyl orange aqueous solution with low concentration, its photocatalytic decolorization is a pseudo-first-order reaction and its kinetics may be expressed as $\ln(c_0/c) = kt$, where k is the apparent rate constant, and c_0 and c are the initial and reaction concentrations of aqueous methyl orange, respectively.[13]

3. Results and Discussion

3.1. Thermal Analysis. Figure 1 shows thermogravimetry (TG) curve of TiO_2 powder sample obtained by LPD method. The TG curve can be roughly divided into three stages. The first stage is from room temperature to 250 °C, a mass loss of about 8.44% is observed, which can be attributed to the evaporation of the physically adsorbed water and other chemicals. The largest weight loss (45.14%) occurs in the temperature range from 250 to 575 °C. This is attributed to the thermal decomposition of some intermediate compounds containing NH_4^+ and F^- in the TiO_2 powders.[15] The third stage is from 575 to 1000 °C, where the mass loss is about 1.43%. This can be assigned to the dehydration and evaporation of chemisorbed water.

3.2. FT-IR Spectroscopy. FT-IR spectra of the TiO_2 powder samples calcined at various temperatures are shown in Figure 2. The TiO_2 samples show the main bands at 400−700 cm^{-1}, which are attributed to Ti−O stretching and Ti−O−Ti bridging

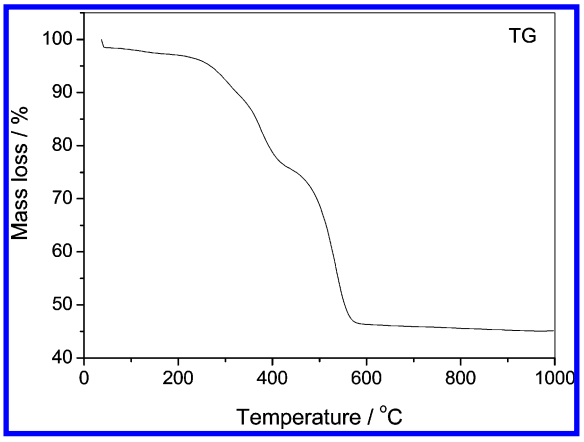

Figure 1. TG curve of TiO_2 powder prepared by LPD.

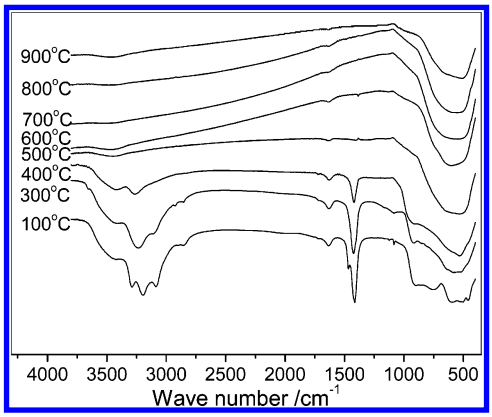

Figure 2. Infrared spectra of TiO_2 powder calcined at various temperatures.

stretching modes.[25] The bands at 700−900 cm^{-1} are attributed to Ti−F vibration.[26] The regions of 1400−1750 cm^{-1} are attributed to bending vibrations of O−H and N−H. The broad bands at 2800−3800 cm^{-1} are assigned to the O−H vibration for water molecules and Ti−OH and the N−H vibration for NH_4^+ ions.[27,28] The IR spectra of the sample dried at 100 °C reveal that Ti−O, Ti−F, N−H, Ti−OH, H−O−H groups exist in the as-prepared sample by the LPD method. Since LPD process is performed in the aqueous solution system, the films easily absorb water molecules, NH_4^+, and F^- ions in the treatment solution. The intensities of O−H, N−H, and Ti−F vibration bands decrease and the intensities of Ti−O vibration bands increase with increasing calcination temperature, also impurities almost completely disappear after calcination at 500 °C. This is in good agreement with the TG results. It has been shown that the removal of impurity groups promotes the rearrangement of the Ti−O network and the crystallization of titania at 500 °C. When the calcination temperature is over 500 °C, there are also some small vibration bands in the Figure 2. At 900 °C, a very small peak at about 1620 cm^{-1} also exists, which corresponds to the hydroxyl groups in TiO_2 thin films. It can be concluded from the TG and FTIR results that the hydroxyl groups in TiO_2 thin films can never be completely removed.

3.3. XRD Study. XRD results show that all as-prepared precursor TiO_2 thin films by the above-described method were amorphous, which differs from TiO_2 thin films prepared by the controlled hydrolysis method.[29] The hydrolysis of $TiCl_4$,[30−34] TiF_4,[35,36] or $(NH_4)_2TiF_6$[16,24,37,38] can yield either amorphous or crystallized TiO_2 thin films, depending on the hydrolysis conditions employed. A solution with lower precursor concentration or higher molar ratio of H_2O/precursor usually favors the formation of crystallized TiO_2 thin films.[16,29] This is probably due to the fact that, with increasing water content, a stronger nucleophilic reaction between H_2O and TiF_6^{2-} ions occurs and more F^- ions in the TiF_6^{2-} ions will be substituted by the hydroxyl groups. Therefore, the decrease of the quantity of unhydrolyzed F^- ions in precursors results in the enhancement of TiO_2 crystallization to crystalline anatase**.** Hydrolysis reactions of $(NH_4)_2TiF_6$ in the presence of H_2O can be represented as follows:[29]

TABLE 1: Effects of Calcination Temperature on Phase Structure and Average Crystallite Size (nm) of TiO_2 Thin Films[a]

	100 °C	500 °C	700 °C	900 °C
D_A	0	14.5	41.1	72.3
D_R	0	0	0	77.1

[a] D_A and D_R denote the average crystallite size of anatase and rutile in TiO_2 thin films.

$$[TiF_6]^{2-} + nH_2O \rightleftharpoons [TiF_{6-n}(OH)_n]^{2-} + nHF \quad (1)$$

$$[TiF_{6-n}(OH)_n]^{2-} \xrightarrow{H_2O}$$

$$[TiF_{5-n}(OH)_{n+1}]^{2-} + H^+ + F^- \xrightarrow{(5-n)H_2O}$$

$$[Ti(OH)_6]^{2-} + (6-n)F^- + (6-n)H^+ \quad (3)$$

$$[Ti(OH)_6]^{2-} + 2H^+ \rightarrow TiO_2 + 4H_2O \quad (4)$$

Of course, raising the hydrolysis temperature is also beneficial to the crystallization of TiO_2 due to the accelerating of hydrolysis reactions of TiF_6^{2-} ions. However, a low precursor concentration is unsuitable for the preparation of thick TiO_2 thin films using the above-described method. Moreover, the TiO_2 anatase thin films obtained by the controlled hydrolysis method at room-temperature always have poor photocatalytic activity due to the weak crystallization and the presence of impurities. Therefore, the TiO_2 thin films photocatalyst obtained by the LPD method must be heat-treated at high temperatures in order to remove impurities and enhance crystallization.

The XRD results of TiO_2 thin films deposited on quartz indicate that the TiO_2 thin films calcined at 500 and 900 °C show the some preferential orientation for anatase in the (101) direction and rutile in the (110) direction, respectively. The corresponding XRD patterns for the TiO_2 thin films calcined at 500, 700, and 900 °C are provided in the Supporting Information (Figure S1). At 500 °C, the width of the anatase (101) plane diffraction peak ($2\theta = 25.40°$) shows wider, which indicates the formation of fine crystallites in the film. With increasing calcination temperature, the peak intensity of anatase increases and the width of the (101) peak becomes narrower, which is due to the growth of crystallites and improvement of crystallization. At 900 °C, the thermodynamically favored rutile phase begins to form and becomes a main phase. The films contain two phases of anatase and rutile, and their crystallite size increases greatly due to the phase transformation of anatase to rutile. The average crystallite sizes of the TiO_2 films calculated using Scherrer's equation for the main diffraction peak are shown in Table 1. When the calcination temperature is below 500 °C, there are no diffraction peaks and thin films appear in the amorphous state. This may be ascribed to the fact that the films calcined at below 500 °C are composed of amorphous titania or the amount of anatase is too low. This suggests that the phase transformation from amorphous to anatase in the films

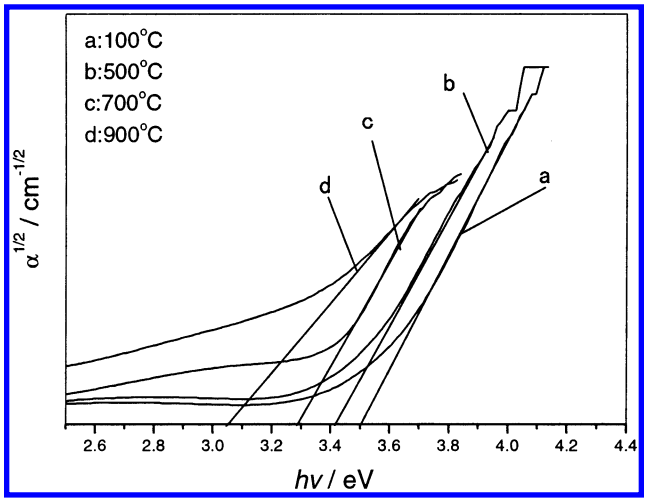

Figure 3. Plots of $\alpha^{1/2}$ versus photon energy ($h\nu$) for the TiO_2 thin films calcined at 100 (a), 500 (b), 700 (c), and 900 °C (d).

occurs at ca. 500 °C. This agrees with the results of TG and FT-IR, which show that almost all impurities preventing crystallization were completely removed from the films at 500 °C. The phase transformation temperature of amorphous to anatase seems to be slightly higher than that observed for the TiO_2 thin film prepared by sol−gel method (about 400 °C).[12,13] This is ascribed to the fact that the ligands suppress the formation of ordered metal−oxygen networks and prevent the crystallization of TiO_2 within the thin films due to the existence of strong titanium complexing ions such as F^- ions.[22,39]

The phase transformation temperature of anatase to rutile is also increased due to the presence of SiO_2 in the films.[40,41] For pure TiO_2 samples, the rutile phase begins to form at 700 °C, and the anatase is completely transformed to rutile by 900 °C.[11] This is ascribed to the stabilization of the anatase phase by the surrounding SiO_2 phase through the TiOSi interface. At the interface, Ti atoms are substituted into the tetrahedral SiO_2 lattice forming tetrahedral Ti sites. The interaction between the tetrahedral Ti species and the octahedral Ti sites in the anatase is thought to prevent the transformation to rutile.[40,42] The SiO_2 lattice locks the Ti−O species at the interface of the TiO_2 domains, preventing the nucleation that is necessary for the phase transformation to rutile. Hence, greater heat is required to drive the crystallization.[40,42]

3.4. UV−Vis Spectra. The TiO_2 thin films deposited on fused quartz and calcined at various temperatures are transparent. The corresponding UV−Vis spectra for the TiO_2 thin films calcined at 100, 500, 700, and 900 °C are provided as Supporting Information (Figure S2). A significant decrease in the transmittance below 400 nm can be assigned to absorption of light caused by the excitation of electrons from the valence band to the conduction band of titania. The transmittance of titania thin films calcined at below 700 °C is about 60% over the visible light spectra region and is slightly lower than that of the TiO_2 thin films obtained by the sol−gel method.[12,13] This can be ascribed to the formation of larger spherical particles with several hundreds nanometers in diameter on the surface of TiO_2 thin films (according to Figure 4), which causes the scattering of light. With increasing calcination temperature, the changes in the transmittance and absorption edge wavelength of the TiO_2 thin films are ascribed to the difference in surface morphologies, crystallite size, phase structure, and compositions within the films. When the calcination temperature is below 700 °C, the "red-shift" of absorption edge wavelength can be attributed to the growth of TiO_2 crystallites. At 900 °C, the "red-shift" is due to the phase transformation from anatase to rutile, leading to the decrease of band gap energy. The decrease in transmittance of the film is due to the fact that the film is mainly composed of rutile, which has a more intense absorbance than anatase in the visible region.[43,44] Also, the existence of surface cracks in the film will result in the decrease of the transmittance due to scattering of light.[45,46]

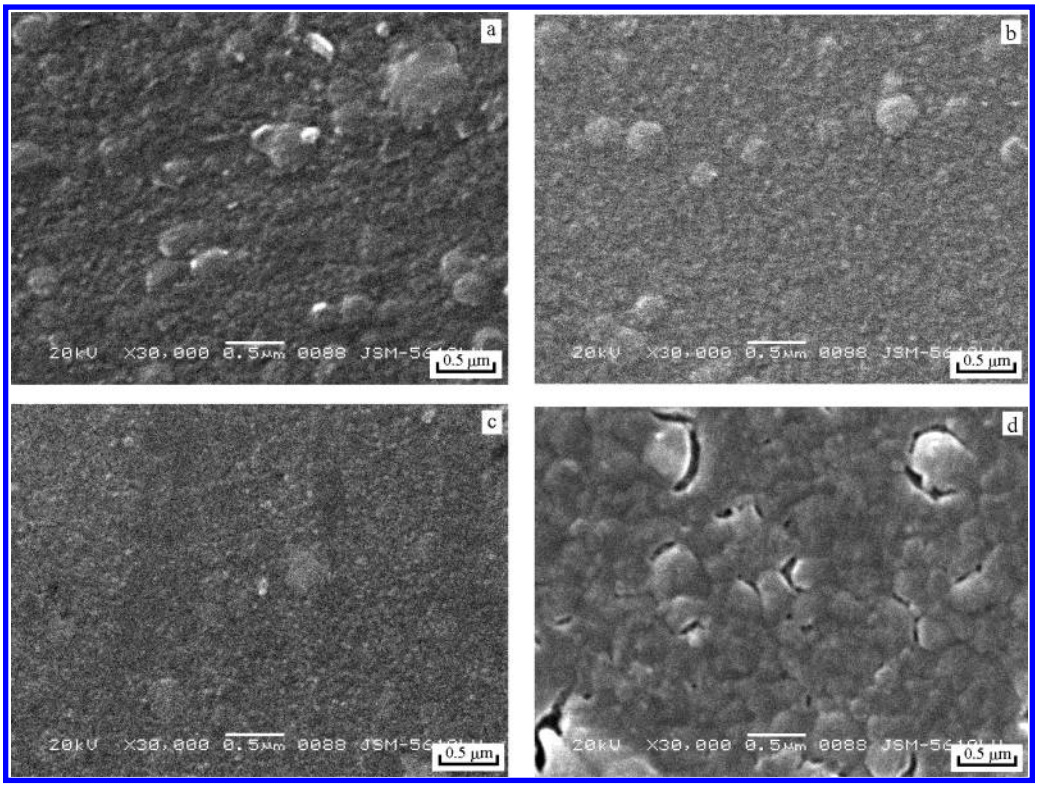

Figure 4. SEM micrographs of TiO_2 films calcined at 100 (a), 500 (b), 700 (c), and 900 °C (d).

The difference in absorption edge wavelength for the TiO_2 thin films clearly indicates a decrease in the band gap of TiO_2 with increasing calcination temperature. To have a quantitative estimate of the band gap energies, the absorption coefficient α of the thin films, near the absorption edge, was calculated from the transmittance T and reflectance R data using the simplified relation $T = (1 - R)^2e^{-\alpha d}/(1 - R^2e^{-2\alpha d})$, where d is the thickness of films.[43,44] The intercepts of the tangents to the $\alpha^{1/2}$ versus photon energy ($h\nu$) plots will give an estimate of the band gap energies of TiO_2 thin films. Plots of $\alpha^{1/2}$ versus photo energy ($h\nu$) for TiO_2 thin films calcined at 100, 500, 700, and 900 °C are shown in Figure 3. The band gap energies for TiO_2 films calcined at 100, 500, 700, and 900 °C are estimated to be 3.50, 3.42, 3.29, and 3.06 eV, respectively. The band gap energies for TiO_2 films calcined at 500, 700, and 900 °C are larger than the band gap energies of anatase and rutile TiO_2 ($E_g = 3.2$ and 3.0 eV), respectively, which may be attributed to the thermal stress in the film due to the difference in the thermal expansion coefficients between the substrate and the TiO_2 film.[47] Furthermore, the difference between the band gap energies of TiO_2 thin films calcined at 500 and 700 °C may be due to the difference in crystallite size (as shown in Table 1).[12,13]

3.5. SEM Analysis. Figure 4 shows SEM micrographs of the TiO_2 thin films deposited on quartz and calcined at 100 (a), 500 (b), 700 (c), and 900 °C (d), respectively. It can be observed that the surface morphologies and roughness of the TiO_2 thin films are obviously different at different calcination temperatures. At 100 °C, the film consists of spherical particles with a large diameter range from 60 to 400 nm and there are some impurities on the surface of thin film. This is due to the fact that the particle size and its distribution are affected by the rates of nucleation and growth. If the nucleation rate is much greater than the rate at which the new precursor is generated, nucleation does not occur simultaneously with the growth, and particles with narrow size distribution can be obtained. Conversely, if the nucleation rate is not high enough compared to the rate of precursor generation, the precursor concentration remains higher than a critical concentration C_{min}, and nucleation and growth occur simultaneously. The older nuclei will grow to be larger than the younger ones, leading to a wide grain-size distribution.[29] It can be inferred from the above these research that at the beginning of the hydrolysis reaction, the nucleation rate is much greater than the growth rate due to a high precursor concentration. With increasing reaction time, the nucleation rate is slow and the growth rate accelerates due to the decrease in precursor concentration. The nucleation and growth occur simultaneously, which results in a wide particle size distribution.[29] Therefore, the LPD-derived oxide thin films are usually composed of different sized particles.

When the calcination temperature is not above 700 °C, with increasing calcination temperature, the surface morphology and roughness of the TiO_2 thin films do not alter obviously, but the thin film becomes denser and some impurities disappear. At 900 °C, the surface morphology and roughness of the thin films occur to change significantly. The thin film is composed of unspherical particles of ca. 200 to 600 nm in diameter, which is caused by the phase transformation from anatase to rutile and growth of TiO_2 crystallites. Furthermore, some cracks are observed, which may be ascribed to the increase of internal stress with the shrinkage of thin film. It can be inferred from the previous XRD results that the particles in TiO_2 thin films are some aggregates of many small TiO_2 crystallites. The thickness of TiO_2 thin films calcined at different temperature is observed with SEM. The corresponding cross-sectional SEM images for the TiO_2 thin films calcined at 700 and 900 °C are provided as Supporting Information (Figure S3). The dense and uniform titania thin film can be obtained after calcination at 700 °C. At 900 °C, the thickness is not uniform. Also there are some gaps on the cross-sectional surface, which are due to the formation of some cracks in the thin film. The thickness of TiO_2 thin films calcined at 500, 700, and 900 °C is ca. 300, 250, and 220 nm, respectively.

The formation mechanisms of the LPD-deposited TiO_2 thin films may be accounted for qualitatively by the pH of treatment solution relative to the isoelectric points of TiO_2 and SiO_2.[16] The pH (3.9) of the treatment solution is below the isoelectric point of TiO_2 (reported values were 5.6,[48] 5.9,[49] and 6.2[50]). TiO_2 forming under these conditions will therefore have a positive surface charge density and would be expected to experience a significant electrostatic attraction to surfaces with negative surface charge density.[16] Reported values of the isoelectric point of SiO_2 range from 1.8[51] to 2.7.[52] This means that the quartz surface is negatively charged at pH 4. Thus TiO_2 thin films were deposited by the electrostatic attraction between TiO_2 and SiO_2. We found that the pH is an important parameter for controlling the quality of thin films obtained by the LPD method. With decreasing the pH (from 3.9 to 2.8), the quality of TiO_2 thin films become poor probably due to the weak electrostatic attraction between TiO_2 and SiO_2. With further decreasing the pH (from 2.8 to 1.8), the TiO_2 thin films cannot form, probably due to the repulse interaction between TiO_2 and SiO_2 or low supersaturation. With increasing the pH (from 3.9 to 5.0), a large amount of TiO_2 powders are produced by homogenerous nucleation due to a high degree of supersaturation, causing the adhesion power of the thin films to drop.

3.6. Photoluminescence Spectra. The PL emission spectra can be useful to disclose the efficiency of charge carrier trapping, immigration, and transfer, and to understand the fate of electrons and holes in semiconductor since PL emission results from the recombination of free carriers.[53−55] To the best of our knowledge, it is difficult to observe any photoluminescence phenomenon at room temperature for bulk TiO_2, even in the monocrystal state, due to its indirect transition nature.[56,57] On the contrary, some nanometer-sized TiO_2 particles and mesoporous structured TiO_2 powders have been reported to exhibit room-temperature photoluminescence. For example, Zou et al.[56] reported room-temperature photoluminescence of TiO_2 ultrafine particles coated with stearic acid and attributed this phenomenon to the modification of stearic acid on the TiO_2 surface. Bai et al.[57] also reported the room-temperature photoluminescence properties of mesolamellar TiO_2 films. Very recently, we also reported the room-temperature photoluminescence properties of mesoporous TiO_2 powders and thin films.[11,58] Figure 5 shows the room temperature photoluminescence spectra for TiO_2 thin films calcined at 500, 700, and 900 °C in the range of 350−550 nm. Two main emission peaks appear at about 367 and 473 nm wavelengths, which are equivalent to the 3.38 and 2.62 eV, respectively. The former is ascribed to the emission of band gap transition.[55] The latter is emission signal originated from the charge-transfer transition from Ti^{3+} to oxygen anion in a TiO_6^{8-} complex.[11,55] The difference of about 0.8 eV between the band gap energy (3.4 eV for anatase, as shown in Figure 3) and the emission peak energy (2.6 eV) is caused by the Stokes shift due to the Franck−Condon effect.[11,59,60]

The variation of PL intensity may result from the change of defect state on the shallow level of the TiO_2 surface.[54,61] The difference of PL spectra in Figure 5 is due to various calcination temperatures leading to different phase structure and surface

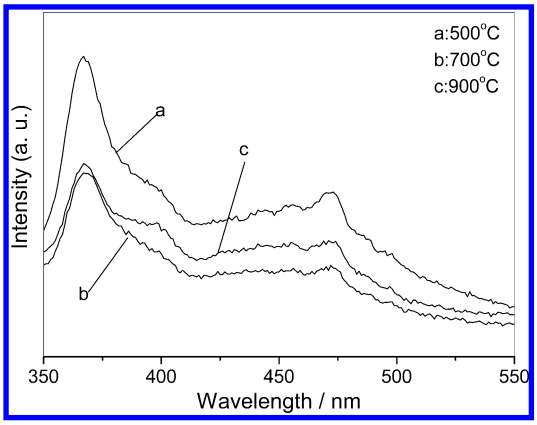

Figure 5. The photoluminescence spectra for TiO_2 thin films calcined at 500 (a), 700 (b), and 900 °C (c).

TABLE 2: Composition (at. %) of TiO_2 Thin Films Calcined at Various Temperatures According to XPS Analysis

	films				
temperature	O	Ti	F	Si	N
100 °C	67.8	25.1	3.2	1.7	2.2
500 °C	68.9	25.7	0.6	1.9	2.9
700 °C	70.8	20.7	0	7.3	1.2
900 °C	69.4	20.8	0	7.5	2.3

microstructure. The sample calcined at 500 °C shows high emission intensity. With increasing calcination temperature, there is a significant decrease in the intensity of PL spectra. The PL emission mainly results from the recombination of excited electrons and holes, and the lower PL intensity indicates the decrease in recombination rate.[53−55] At 700 °C, the lowest PL intensity was observed due to the TiO_2 thin film with better crystallization. At 700 °C, Si cannot enter the lattice of TiO_2 to form solid solution. Therefore, the increase in the amount of SiO_2 has little effect on the PL intensity. At 900 °C, the PL emission intensity of thin film increases slightly, which may be due to the introduction of new defect sites (such as the formation of a SiOTi solid solution) and cracks in the thin film.[11]

3.7. XPS Studies. The compositions of TiO_2 thin films calcined at 100, 500, 700, and 900 °C were characterized with XPS. The corresponding XPS survey spectra for the TiO_2 thin films calcined at 100, 500, 700, and 900 °C are provided as Supporting Information (Figure S4). The XPS results show that TiO_2 thin films deposited on quartz contain not only Ti and O elements, but also some F, N, and Si elements. The XPS peak for C1s at $E_b = 284.8$ eV is observed due to the adventitious hydrocarbon from the XPS instrument itself. The XPS peaks for F and N are observed in the spectra, which are due to the residual elements from precursor solution. The high-resolution XPS spectra of the F1s region for TiO_2 thin films calcined at 100, 500, and 700 °C show that the peak intensities for F1s decrease significantly and disappear when the calcination temperature reaches 700 °C, which means that the F element in the thin films gradually evaporates with increasing calcination temperature. The corresponding high-resolution XPS region spectra for the TiO_2 thin films calcined at 100, 500, and 700 °C are provided as Supporting Information (Figure S5). Table 2 shows the composition (at. %) of TiO_2 thin films calcined at various temperatures according to XPS analysis. It can be seen that the amount of F element in the film calcined at 100, 500, and 700 °C is about 3.2, 0.6, and 0%, respectively.

The photoelectron peak of Si2p appears at a binding energy of 102.5 eV. It is well-known that XPS is a surface probe detecting electrons that are generated from a depth of a few nanometers on the surface of the sample. The thickness of the thin films in our experiment is over 220 nm, which is much larger than the depth that XPS could detect. Moreover, the film samples calcined at below 700 °C are dense and do not fracture according to the previous SEM observation. It can be inferred that the photoelectron peak for Si2p comes from the thin film itself, not from the fused quartz substrate. In our experiment, there is no Si element in the treatment solution. We only use a glass beaker as a container and fused quartz as a substrate. To clarify the source of the Si element, we also use the plastic beaker instead of a glass beaker as a container. The results show that there is some Si element in the XPS survey spectra for the as-prepared TiO_2 thin film; similar results were also reported by Lee at al.[62] They found that the TiO_2 thin films deposited on the silicon substrate from a saturation solution of hexafluorotitantic acid contain SiO_2. Herein, though we use ammonium hexafluorotitanate as a precursor instead of hexafluorotitantic acid, there also exists that phenomenon. According to eq 1, the LPD process consists of a ligand exchange equilibrium reaction, so there exists some HF in the solution. It is well-known that HF can easily react with SiO_2 to form stable SiF_6^{2-} ions in aqueous solution. We conclude that there is another equilibrium reaction in the solution as follows:

$$4H^+ + SiO_2 + 6F^- \rightleftharpoons SiF_6^{2-} + 2H_2O \qquad (5)$$

The fused quartz immersed in the treatment solution can react with the solution to form SiF_6^{2-} ions, leading to the TiO_2 thin films containing some SiO_2. Table 2 shows that the amount of Si element on the surface of the thin film sample increases significantly after calcination at 700 °C. The significant increase of SiO_2 in the thin film can be due to the diffusion of Si element from the surface of the quartz substrate into the TiO_2 thin film. It is well-known that the quartz substrate is quite stable and inert, and it is difficult for SiO_2 to diffuse due to the ordered silicon−oxygen networks. In our study, the reaction of quartz substrate with the treatment solution can lead to the destruction of ordered silicon−oxygen networks on the surface of quartz, which makes it possible for a large amount of Si element to diffuse from the surface of quartz into the thin film to form SiO_2/TiO_2 composite thin films at 700 °C or higher temperature. Further observation from Table 2 shows that the amount of SiO_2 does not increase significantly at 900 °C. This may be attributed to the destroyed (or etched) layer on the surface of quartz almost completely diffused into TiO_2 thin films at 700 °C; consequently, the amount of Si element on the surface of the thin film sample at 900 °C does not increases greatly. According to the above results, at 500 °C or lower temperature, a small amount of SiO_2 in the thin films comes from the SiF_6^{2-} ions in treatment solution. However, at 700 °C or higher temperature, the increasing amount of SiO_2 in the thin films can be mainly attributed to the diffusion of Si element from the surface of quartz into the thin film. This shows that the diffusion of Si element from quartz into the thin film mainly occurs at ca. 700 °C.

Figure 6 shows the high-resolution XPS spectra of the O1s region, taken on the surface of TiO_2 thin films calcined at 100, 500, 700, and 900 °C, respectively. The O1s region is decomposed into three contributions. The main contribution is attributed to Ti−O in TiO_2, and the other two kinds of oxygen contributions can be ascribed to the OH in Ti−OH and the Si−O in SiO_2, respectively. Although some H_2O is easily adsorbed on the surface of TiO_2 films during deposition process, the physically absorbed H_2O on TiO_2 is easily desorbed under the

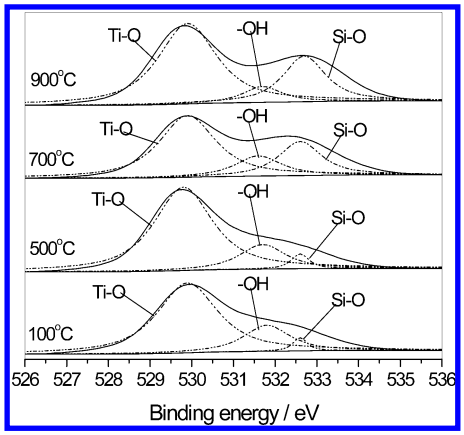

Figure 6. High-resolution XPS spectra of the O1s region of the TiO_2 thin films calcined at 100, 500, 700, and 900 °C.

TABLE 3: Results of Curve-Fitting of High-Resolution XPS Spectra for the O1s Region of TiO_2 Thin Films

films		O1s (Ti−O)	O1s (OH)	O1s (O−Si)
TiO_2/SiO_2 + (100 °C)	E_b/eV	529.9	531.8	532.5
	fwhm	1.66	1.30	0.50
	r_i/%	75.32	21.32	3.36
TiO_2/SiO_2 + (500 °C)	E_b/eV	529.9	531.8	532.5
	fwhm	1.66	1.30	0.50
	r_i/%	77.83	18.00	4.17
TiO_2/SiO_2 + (700 °C)	E_b/eV	529.9	531.7	532.5
	fwhm	1.66	1.30	1.20
	r_i/%	63.65	12.73	23.62
TiO_2/SiO_2 + (900 °C)	E_b/eV	529.9	531.6	532.5
	fwhm	1.66	1.10	1.20
	r_i/%	66.81	6.53	26.66

ultrahigh vacuum condition of the XPS system. Therefore, the hydroxyl on the surface can be attributed to the Ti−OH on the thin films. Table 3 lists the results of curve fitting of XPS spectra for TiO_2 film samples calcined at 100, 500, 700, and 900 °C. It can be seen from the Table 3 and Figure 6 that the hydroxyl content of the samples decreases with increasing calcination temperature, which is due to the fact that there is a reaction on the surface of TiO_2 thin films during the calcination process: Ti−OH + HO−Ti → Ti−O−Ti + H_2O. At 900 °C, the TiO_2 thin films still contain a small amount of hydroxyl. This is probably due to the fact that the films easily adsorb water vapor in air, leading to the formation of hydroxyl on the films. This also corresponds to the results of previous TG and FTIR. According to Table 3, the amount of Si−O in the thin film increases significantly when the calcination temperature is over 700 °C, which is caused by the diffusion of Si element from the surface of quartz substrate into the TiO_2 thin film.

3.8. Photocatalytic Activity of the TiO_2 Thin Films. The photocatalytic activity of the thin films was evaluated by photocatalytic decolorization of methyl orange aqueous solution. However, under dark conditions without light illumination, the content of methyl orange does not change for every measurement using various TiO_2 thin films. Illumination in the absence of TiO_2 films does not result in the photocatalytic decolorization of methyl orange. Therefore, the presence of both illumination and TiO_2 films is necessary for the efficient degradation. These results also suggest that the degradation decolorization of methyl orange aqueous solution is caused by photocatalytic reactions on TiO_2 thin films under the UV illumination.

Figure 7 shows the relationship between the apparent rate constants of methyl orange degradation decolorization and calcination temperatures. There is no photocatalytic activity when the calcination temperature is below 400 °C, which is

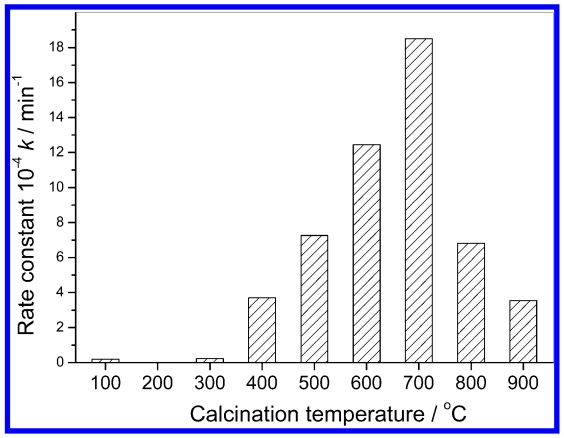

Figure 7. Rate constants for the photocatalytic decomposition of methyl orange on TiO_2 thin films calcined at various temperatures. Initial methyl orange concentration = 1.53×10^{-3} mol L^{-1}, film area = 80 cm^2.

due to the fact that the thin films are composed of amorphous TiO_2. With increasing calcination temperature, the photocatalytic activity of thin films increases and reaches the maximum value at 700 °C. The increase in photocatalytic activity is due to the formation of anatase and the improvement of crystallization of anatase in the films.

It can be seen from Figure 7 that the TiO_2 film calcined at 700 °C shows the highest photocatalytic activity, which is 2.5 times that of the thin film sample calcined at 500 °C. It was reported that a mixed oxide of TiO_2 and SiO_2 produced by a sol−gel method was a more efficient photocatalyst for the photocatalytic decomposition of rhodamine-6G (R-6G) than TiO_2 alone in aqueous solution.[40] The increase in efficiency was attributed to the presence of an adsorbent (SiO_2). The adsorbent phase increased the concentration of R-6G near the TiO_2 sites relative to the solution concentration.[40] In this work, we found that there was much more silicon dioxide in the films (according to the XPS results, as shown in Table 3) at 700 °C than below 700 °C. This means that the increasing amount of SiO_2 in the thin film can form an adsorption center for methyl orange. The TiO_2 behaves as the photoactive center, e.g., generating hydroxyl radicals under UV irradiation, while the SiO_2 provide better adsorption sites in the vicinity of the TiO_2. Of course, the calcined thin film at 700 °C shows better crystallization, which is also beneficial to the enhancement of photocatalytic activity. All these factors contribute to an enhancing photocatalytic activity. Miyashita et al.[63] have found that the presence of longer-lived photogenerated charge carriers at the SiO_2/TiO_2 interface was observed, where the nanometer-scale SiO_2 overlayer suppresses the recombination of electron−hole pairs, leading to higher photocatalytic activity. Many other researchers[64−66] also found that the addition of silica increased the photocatalytic activity. Li et al.[53−55] thought that the lower PL intensity can be ascribed to the lower recombination rate of photogenerated electrons and holes under light irradiation, which leads to the higher photocatalytic activity of the sample. At 700 °C, the lowest PL intensity for the TiO_2 thin film was observed. This sample also has the highest photocatalytic activity.

It is well-known that titania has three different crystalline phase: anatase, rutile, and brookite, and the rutile has the lowest photocatalytic activity. The decrease in the phtotcatalytic activity of the thin films calcined at above 700 °C is due to the following factors. First, according to XRD results, the phase transformation of anatase to rutile occurred at about 900 °C and the thin film is mainly composed of rutile. Second, the sintering and growth

of TiO_2 crystallites result in the significant decrease of surface area of the TiO_2 thin films. Also, the phase transformation from anatase to rutile further accelerates the growth of crystallites by providing the heat of phase transformation.[11] These causes may result in the rapid decrease in photocatalytic activity.

4. Conclusions

By the LPD method, the dense and uniform titania thin films can be deposited on quartz substrate. The as-prepared TiO_2 thin films contain not only Ti and O elements, but also some F, N, and Si elements. The F and N elements come from the precursor solution, and the amount of F element decreases with increasing calcination temperature. The Si element in the TiO_2 thin films can be divided into two contributions. One is from the SiF_6^{2-} ions in the treatment solution. The other is attributed to the diffusion of Si element from the surface of quartz substrate into thin films at 700 °C or higher temperatures. The TiO_2 thin films show the obviously preferential orientation for anatase in the (101) direction at 500 °C and rutile in the (110) direction at 900 °C.

The photocatalytic activity of TiO_2 thin films deposited on quartz strongly depends on the calcination temperature. When the calcination temperature is below 400 °C, there is no photocatalytic activity because the thin films are composed of amorphous TiO_2. With increasing calcination temperature, the photocatalytic activity increases due to the formation of anatase TiO_2 and the improvement of crystallization. At 700 °C, the TiO_2 thin film shows the highest photocatalytic activity due to the increasing amount of SiO_2 as an adsorbent center and better crystallization of TiO_2 in the SiO_2/TiO_2 composite thin film. Moreover, the SiO_2/TiO_2 composite thin film shows the lowest PL intensity due to the decrease in the recombination rate of photogenerated electrons and holes under UV light irradiation. When the calcination temperature is over 700 °C, the photocatalytic activity of thin films decreases, which is due to the formation of rutile and the sintering and growth of TiO_2 crystallites resulting in the decrease of surface area.

Acknowledgment. This work was partially supported by the National Natural Science Foundation of China (50272049). This work was also financially supported by the Excellent Young Teachers Program of MOE of China and Project-Sponsored by SRF for ROCS of SEM of China.

Supporting Information Available: Figures S1−S5, showing XRD patterns, UV−Visible tansmittance spectra, cross-sectional SEM images, XPS survey, and high-resolution spectra of TiO_2 films calcined at different temperatures, respectively. This material is available free of charge via the Internet at http://pubs.acs.org.

References and Notes

(1) Honda, K.; Fujishima, A. *Nature* **1972**, *238*, 37.
(2) Linsebigler, A. L.; Lu, G.; Yates, J. T., Jr. *Chem. Rev.* **1995**, *95*, 735.
(3) Tada, H.; Yamamoto, M.; Ito, S. *Langmuir* **1999**, *15*, 3699.
(4) Liu, H.; Cheng, S.; Wu, M.; Wu, H.; Zhang, J.; Li, W.; Cao, C. *J. Phys. Chem. A* **2000**, *104*, 7016.
(5) Li, X. Z.; Li, F. B. *Environ. Sci. Technol.* **2001**, *35*, 2381.
(6) Hoffmann, M. R.; Martin, S. T.; Choi, W.; Bahnemann, D. W. *Chem. Rev.* **1995**, *95*, 69.
(7) Fu, X. Z.; Clark, L. A.; Yang, Q.; Anderson, M. A. *Environ. Sci. Technol.* **1996**, *30*, 647.
(8) Zhao, J. C.; Wu, T. X.; Wu, K. Q.; Oikawa, K.; Hidaka, H.; Serpone, N. *Environ. Sci. Technol.* **1998**, *32*, 2394.
(9) Xu, Y. M.; Langford, C. H. *Langmuir* **2001**, *17*, 897.
(10) Yu, J. C.; Yu, J. G.; Ho, W. K.; Zhang, L. Z. *Chem. Commun*. **2001**, 1942.
(11) Yu, J. C.; Yu, J. G.; Ho, W. K.; Zhang, L. Z. *Chem. Mater*. **2002**, *14*, 3808.
(12) Yu, J. C.; Yu, J. G.; Zhao, J. C. *Appl. Catal.* B: *Environ.* **2002**, *36*, 31.
(13) Yu, J. G.; Zhao, X. J. *Mater. Res. Bull.* **2001**, *36*, 97.
(14) Nagayama, H.; Honda, H.; Kawahara, H. *J. Electrochem. Soc.* **1988**, *135*, 2013.
(15) Niesen, T. P.; De Guire, M. R. *J. Electroceram*. **2001**, *6*, 169.
(16) Pizem, H.; Sukenik, C. N.; Sampathkumaran, U.; Mcllwain, A. K.; De Guire, M. R. *Chem. Mater*. **2002**, *14*, 2476.
(17) Masuda, Y.; Ieda, S.; Koumoto, K. *Langmuir* **2003**, *19*, 4415.
(18) Dutschke, A.; Diegelmann, C.; Lobmann, P. *J. Mater. Chem.* **2003**, *13*, 1058.
(19) Wang, X. P.; Yu, Y.; Hu, X. F.; Gao, L. *Thin Solid Films* **2000**, *371*, 148.
(20) Schmitt, R. H.; Glove, E. L.; Brown, R. D. *J. Am. Chem. Soc.* **1960**, *82*, 5292.
(21) Wamser, C. A. *J. Am. Chem. Soc.* **1951**, *73*, 409.
(22) Kishimoto, H.; Takahama, K.; Hashimoto, N.; Aoi, Y.; Deki, S. *J. Mater. Chem*. **1998**, *8*, 2019.
(23) Deki, S.; Aoi, Y.; Okibe, J.; Yangimoto, H.; Kajinami, A.; Mizuhata, M. *J. Mater. Chem.* **1997**, *7*, 1769.
(24) Deki, S.; Aoi, Y.; Hiroi, O.; Kajinami, A. *Chem. Lett.* **1996**, *6*, 433.
(25) Peiro, A. M.; Peral, J.; Domingo, C.; Momenech, X.; Ayllon, J. A. *Chem. Mater.* **2001**, *13*, 2567.
(26) Tsukma, K.; Akiyama, T.; Yamada, N.; Imai, H. *J. Non-Cryst. Solids* **1998**, *231*, 161.
(27) Ko, H. Y. Y.; Mizuhata, M.; Kajinami, A.; Deki, S. *J. Flourine Chem.* **2003**, *120*, 157.
(28) Macek, M.; Orel, B.; Krasorec, U. O. *J. Electrochem. Soc.* **1983**, *28*, 17.
(29) Gao, Y.; Masuda, Y.; Koumoto, K. *Chem. Mater.* **2003**, *15*, 2399.
(30) Niessen, T. P.; Bill, J.; Aldinger, F. *Chem. Mater*. **2001**, *13*, 1552.
(31) Kavan, L.; Rathousky, J.; Gratzell, M.; Shklover, V.; Zukal, A. *J. Phys. Chem. B* **2000**, *104*, 12012.
(32) Zheng, Y.; Shi, E.; Chen, Z.; Li, W.; Hu, X. *J. Mater. Chem.* **2001**, *11*, 1547.
(33) Cheng, H.; Ma, J.; Zhao, Z.; Qi, L. *Chem. Mater.* **1995**, *7*, 663.
(34) Harada, H.; Ueda, T. *Chem. Phys. Lett.* **1984**, *106*, 229.
(35) Shimizu, K.; Imai, H.; Hirashima, H.; Tsukuma, K. *Thin Solid Films* **1999**, *351*, 220.
(36) Imai, H.; Matsuda, M.; Shimizu, K.; Hirashima, H.; Negishi, N. *J. Mater. Chem.* **2000**, *10*, 2005.
(37) Koumoto, K.; Seo, S.; Sugiyama, T.; Seo, W. S.; Dressick, W. J. *Chem. Mater.* **1999**, *11*, 2305.
(38) Masuda, Y.; Sugiyama, T.; Koumoto, K. *J. Mater. Chem.* **2002**, *12*, 2643.
(39) Kutty, T. R. N.; Vivekanandan, R.; Murugaraj, P. *Mater. Chem. Phys.* **1988**, *19*, 533.
(40) Anderson, C.; Bard, A. J. *J. Phys. Chem. B* **1997**, *101*, 2611.
(41) Kumar, S. R.; Suresh, C.; Vasudevan, A. K.; Suja, N. R.; Mukundan, P.; Warrier, K. G. K. *Mater. Lett.* **1999**, *38*, 161.
(42) Brinker, C. J.; Scherer, G. W. *Sol−Gel Science*; Academic Press: Boston, 1990.
(43) Rahman, M. M.; Krishna, K. M.; Soga, T.; Jimbo, T.; Umeno, M. *J. Phys. Chem. Solids* **1999**, *60*, 201.
(44) Yu, J. G.; Yu, J. C.; Ho, W. K.; Jiang, Z. T. *New J. Chem.* **2002**, *26*, 607.
(45) Yu, J. G.; Zhao, X. J.; Zhao, Q. N. *Thin Solid Films* **2000**, *379*, 7.
(46) Yu, J. C.; Yu, J. G.; Tang, H. Y.; Zhang, L. Z. *J. Mater. Chem.* **2002**, *12*, 81.
(47) Du, Y.; Zhang, M.-S.; Wu, J.; Kang, L.; Yang, S.; Wu, P.; Yin, Z. *Appl. Phys. A* **2003**, *76*, 1105.
(48) Larson, I.; Drummond, C. J.; Chan, D. Y. C.; Grieser, F. *J. Am. Chem. Soc.* **1993**, *115*, 11885.
(49) Wiese, G. R.; Healy, T. W. *J. Colloid Interface Sci.* **1975**, *51*, 427.
(50) Yotsumoto, H.; Yoon, R. H. *J. Colloid Interface Sci.* **1993**, *157*, 426.
(51) Veeramasuneni, S.; Yalamanchili, M. R.; Miller, J. D. *Colloids Surf. A* **1998**, *31*, 77.
(52) Subramaniam, K.; Yiacoumi, S.; Tsouris, C. *Colloids Surf. A* **2000**, *177*, 133.
(53) Li, X. Z.; Li, F. B.; Yang, C. L.; Ge, W. K. *J. Photochem. Photobiol. A* **2001**, *141*, 209.
(54) Li, F. B.; Li, X. Z. *Appl. Catal. A* **2002**, *228*, 15.
(55) Li, F. B.; Li, X. Z. Chemosphere **2002**, *48*, 1103.
(56) Zou, B.; Xiao; L.; Li T.; Zhao, J.; Lai, Z.; Gu, S. *Appl. Phys. Lett*. **1991**, *59*, 1826.
(57) Bai, N.; Li, S. G.; Chen, H. Y.; Pang, W. Q. *J. Mater. Chem*. **2001**, *11*, 3099.

(58) Yu, J. C.; Ho, W. K.; Yu, J. G.; Hark, S. K.; Lu, K. *Langmuir*, **2003**, *19*, 3889.

(59) Fujihara, K.; Izumi, S.; Ohno, T.; Matsumura, M. *J. Photochem. Photobiol. A* **2000**, *132*, 99.

(60) Serpone, N.; Lawless, D.; Khairutdinov, R. *J. Phys. Chem.* **1995**, *99*, 16646.

(61) Toyoda, T.; Hayakawa, T.; Abe, K.; Shigenari, T.; Shen, Q. *J. Lumin.* **2000**, *87*−*89*, 1237.

(62) Lee, M. K.; Lei, B. H. Jpn. *J. Appl. Phys.* **2000**, *39*, L101.

(63) Miyashita, K.; Kuroda, S.; Tajima, S.; Takehira, K.; Tobita, S.; Kubota, H. *Chem. Phys. Lett.* **2003**, *369*, 225.

(64) Lee, B. Y.; Kim, S. W.; Lee, S. C.; Lee, H. H.; Choung, S. J. *Int. J. Photoenergy* **2003**, *5*, 21.

(65) Zhang, Y. H.; Xiong, G. X.; Yao, N.; Yang, W. S.; Fu, X. Z. *Catal. Today* **2001**, *68*, 89.

(66) Ding, Z.; Lu, G. Q.; Greenfield, P. F. *J. Phys. Chem. B* **2000**, *104*, 4815.